ASME 2016 5th Micro/Nanoscale Heat & Mass Transfer International Conference, MNHMT2016, January 3-6, 2016, Biopolis, Singapore (MNHMT2016-6586)

CONJUGATE HEAT TRANSFER IN SINGLE-PHASE WAVY MICROCHANNEL

Nishant Tiwari
Research Scholar
Department of Mechanical Engineering
National Institute of Technology Rourkela
Rourkela, Odisha, India

Manoj Kumar Moharana
Assistant Professor
Department of Mechanical Engineering
National Institute of Technology Rourkela
Rourkela, Odisha, India

Sunil Kumar Sarangi
Professor and Director
Department of Mechanical Engineering
National Institute of Technology Rourkela
Rourkela, Odisha, India

ABSTRACT

A three-dimensional numerical study has been carried out to understand the effect of axial wall conduction in a conjugate heat transfer situation in a wavy wall square cross section microchannel engraved on solid substrate whose thickness varying between 1.2-3.6 mm. The bottom of the substrate (1.8×30 mm^2) is subjected to constant wall heat flux while remaining faces exposed to ambient are assumed to be adiabatic. The vertical parallel walls are considered wavy such that the channel cross section at any axial location will be a square (0.6×0.6 mm^2) and length of the channel is 30 mm. Wavelength (λ) and amplitude (A) of the wavy channel wall are 12 mm and 0.2 mm respectively. Simulations has been carried out for substrate thickness to channel depth ratio ($\delta_{sf} \sim 1 - 5$), substrate wall to fluid thermal conductivity ratio ($k_{sf} \sim 0.34 – 646$) and flow rate ($Re \sim 100$ to 500).

The results show that with increase in flow rate (Re), the hydrodynamic and thermal boundary layers are thinned due to wavy passage and they shifted from the centerline towards the peak which improves the local heat transfer coefficient at the solid-fluid interface. It is also found that after attaining maximum Nu_{avg} at optimum k_{sf}, the slope goes downward with increasing k_{sf} for all set of δ_{sf} and flow rate (Re) considered in this study.

Keywords: Microchannel; Wavy walls; Laminar flow; Conjugate heat transfer; Axial wall conduction.

INTRODUCTION

In microscale thermal devices, the coupling between wall and bulk fluid temperatures plays important role in the overall heat transfer process. The consequence is that the axial conductive heat transfer in the wall cannot be neglected and that, the heat flux at the solid-fluid interface doesn't remain constant irrespective of constant wall heat flux applied at the base of the substrate. Till now many numerical and experimental studies had been performed on conjugate heat transfer problems in laminar flow pertaining to microchannels and microtubes considering heating over the entire length to understand the effect of axial wall conduction. Moharana and co-authors [1-6] had performed detailed numerical simulation and highlighted the effect of axial wall conduction in microchannels under conjugate heat transfer situations. They also thoroughly reviewed axial wall conduction in microchannel systems and highlighted the role of parameters that affect the thermal performance of microchannels. They found that thermal conductivity ratio and relative wall thickness plays a dominant role in conjugate heat transfer process. It is also found that there exist optimum values of conductivity ratio which maximize average Nusselt number over the full channel length.

Wang et al. [7] experimentally studied conjugate heat transfer in trapezoidal shaped (D_h 155 μm) microchannel under fully-heated conditions on one wall and found that the predictions of wall temperatures and local Nusselt numbers are in good agreement with the experimental data.

Zhang et al. [8] numerically studied the effects of wall axial heat conduction in a conjugate heat transfer problem in simultaneously developing laminar flow and heat transfer in straight thick wall of circular tube with constant outside wall temperature. The results show that the heat transfer process is most sensitive to wall-to-fluid conductivity ratio k_{sf}, and when $k_{sf} \leq 25$, the increasing tube thickness and the decreasing k_{sf} could make the inner wall surface approaching the uniform heat flux condition.

Huang et al. [9] performed an experimental investigation with molecule-based temperature sensors Rhodamine B/DI water and Ru(bpy)/dope for the effect of axial wall conduction in microchannel flow. It was found that the local Nu is higher at the entrance compared with the theoretical calculation because more

aggressive temperature rise at the microchannel entrance is observed and half of the temperature increases at 1/8 of channel length of flow Re ~ 15. It also confirms the effect of axial wall conduction on alternating heat transfer behavior in microchannels.

All the existing studies dealing with conjugate heat transfer are based on straight wall channels of different cross-sectional shapes such as circular, rectangular, square and trapezoidal etc. It has been well-known that when liquid flow in a wavy passage, the mixing of fluid layers is better due to secondary flows (Dean Vortices) generated which enhance the heat transfer rate. The concept of wavy passage had been tested by many researchers for heat transfer enhancement study [10-11]. Recently, Rosaguti et al. [12] performed a numerical study in periodic serpentine channels with various cross-section shapes. They found that when the liquid flow through a wavy passage, the Dean vortices and complex flow patterns emerge. The heat transfer performance found to be greatly improved over straight channels with the same cross section.

Geyer et al. [13] had conducted a numerical investigation on fully developed flow in square ducts with serpentine channel path. From the study, it was found that fluid momentum changes as the fluid moving in serpentine path. The effect of moving fluid parallel to the direction of flow creating Dean's vortices that provides strength after each bend and subsequently enhances the heat transfer performance of the fluid.

Gong et al. [14] used raccoon and wavy microchannels to investigate the performance enhancement of laminar fluid flow subjected to constant heat flux boundary condition. The results shows that the channel having faces (crest and trough) parallel (i.e. wavy channel) to each other has an edge in thermal performance over the configuration where faces (crest and trough) opposite (i.e. raccoon channel) to each other.

Sui et al. [15] numerically analyzed laminar liquid flow and heat transfer in wavy microchannels with rectangular cross-section. The results shows that the quantity and location of the vortices changed along the flow direction leading to scattered advection that improves the convective fluid mixing. Thus, the heat transfer performance was much larger than pressure drop penalty. Secondly, relative waviness renders the temperature distribution much more uniform.

Review of the literature revealed that many studies do exists that deal with independent studies of either conjugate heat transfer in straight wall microchannels or thermal performance of wavy wall microchannels. But none of the studies considered conjugate heat transfer in wavy wall microchannel. So, the present work proposes a three dimensional numerical approach to understand the wall conduction effect in wavy microchannels with square cross-section, under constant wall heat flux condition. Based on the axial variation of wall flux (ϕ) and wall temperature (Θ_w), at the solid-fluid interface and bulk fluid temperature (Θ_f), local and average Nusselt

number are predicted for different wall thickness ratio (δ_{sf} ~ 1 - 5) , thermal conductivity ratio (k_{sf} ~ 0.34 – 646) and flow rate (Re ~ 100 to 500).

NUMERICAL SIMULATION

Square cross-section (0.6×0.6 mm^2) microchannel with wavy vertical wall carved on a solid substrate of size 1.8 × 30 mm^2 with varying thickness (1.2-3.6 mm) is considered in the simulation. The wavelength and the amplitude of the wavy vertical are 12 and 0.2 mm respectively. The bottom of the substrate is subjected to constant wall heat flux while remaining faces exposed to ambient are assumed to be adiabatic. Water at 300 K enters the microchannel with uniform velocity. Simulations have been carried out for varying flow rate (Re), substrate thickness and solid thermal conductivity. The variables considered in this simulation are flow Re, solid wall to fluid conductivity ratio (k_{sf}), and substrate thickness below the channel to channel height ratio (δ_{sf}).

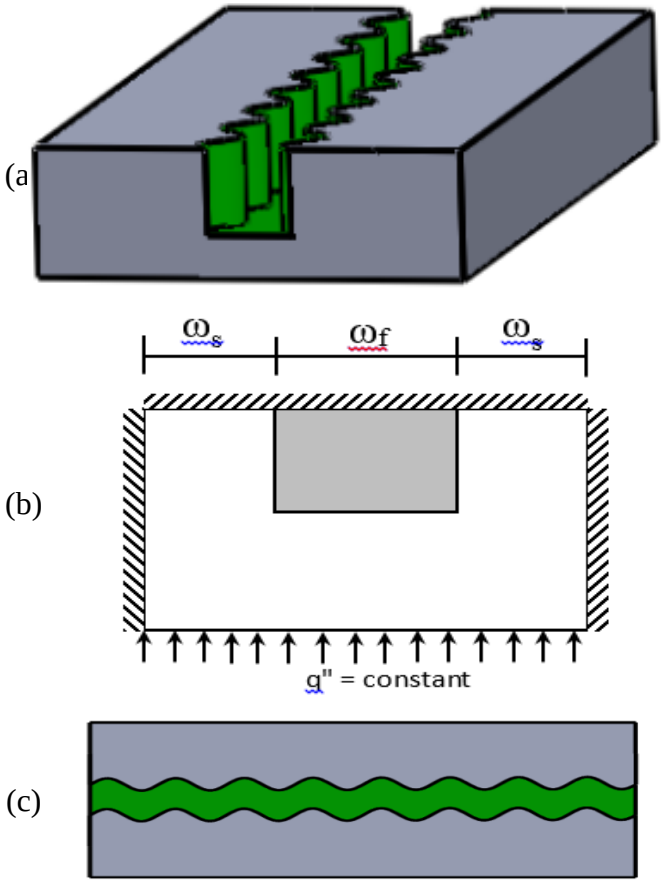

FIGURE 1. (a) WAVY MICROCHANNEL WITH CONDUCTIVE WALL, (b) CROSS-SECTIONAL VIEW, (c) TOP VIEW OF WAVY MICROCHANNEL.

Table 1: Thermo-physical properties of water at the channel inlet of 300K.

Thermo-physical property	Value	Unit
k_f	0.6	W/mK
c_p	4182	j/kg·K
ρ	998.2	kg/m^3
μ	0.001003	kg/m·s

The thermos-physical properties of water at the channel inlet temperature of 300 K is taken from the Fluent database and listed in Table 1. The applied heat flux value is calculated based on temperature rise of the fluid between the inlet and the outlet of 60 K. From calculation, the desired heat flux at the bottom surface of the substrate is found to be 279.52 kW/m^2. A round figure value of 300 kW/m^2 was considered which will result in rise in the fluid temperature to be slightly higher than 60 K. Inlet velocity (u) is uniform which is calculated corresponding to the flow re considered, given by $Re = \rho \cdot u \cdot D_h/\mu$. The uniform water velocity at channel inlet corresponding to flow Re 100 and 500 comes out to be 0.1674 and 1.25 m/s.

The continuity, momentum and energy equations are solved using commercial Ansys-Fluent® software. 'SIMPLE' algorithm is used for pressure velocity coupling, 'Second order upwind scheme' is used for discretization of momentum and energy equations. Pressure interpolation is done using 'standard' scheme. Standard grid independence procedure is adopted to select suitable mesh size. For example, three different grid size of 20×20×100, 24×24×120, and 30×30×150 was used for a wavy vertical square microchannel with negligible wall thickness and local Nusselt number, and pressure drop obtained for a microchannel with negligible wall thickness. The local Nusselt number at the fully developed flow regime changed by 0.55% and the pressure drop changed by less than 1.2% when shifted from the first grid (20×20×100) to third grid size (30×30×150) respectively. So, the middle grid (24×24×120) is selected. Absolute convergence criteria for continuity, energy and momentum equations were taken to be 10^{-6}, 10^{-6} and 10^{-9} respectively.

DATA REDUCTION

The main parameters of interest are (a) peripheral averaged local heat flux (b) local bulk fluid temperature and (c) peripheral averaged local wall temperature. These parameters allow us to determine the extent of axial conduction on the local Nusselt number. The conductivity ratio (k_{sf}) is defined as the ratio of thermal

conductivity of the substrate wall (k_s) to that of the working fluid (k_f). The axial coordinate, z, in non-dimensional form is as follows:

$$z^* = z / L \quad (1)$$

The non-dimensional local heat flux at solid-fluid interface is

$$\phi = q_z / q_i \quad (2)$$

where q_z is the actual local heat flux experienced at the solid-fluid interface along the axial direction of the channel, $q_i = q_a \cdot A_h / A_i$ ideal local heat flux experienced at the solid-fluid interface, q_a is the heat flux applied, A_h is the heating area, A_i is the area of the solid-fluid interface. The dimensionless bulk fluid and microchannel wall temperature, which varies along the axial direction are given by

$$\Theta_f = \frac{T_f - T_{fi}}{T_{fo} - T_{fi}} \quad (3)$$

$$\Theta_w = \frac{T_w - T_{fi}}{T_{fo} - T_{fi}} \quad (4)$$

where, T_{fi} and T_{fo} are the average bulk fluid temperature at the inlet and outlet of the channel respectively, T_f is the average bulk fluid temperature at any location z, and T_w is the wall temperature at the same location. The local Nusselt number is:

$$Nu_z = h_z \cdot D_h / k_f \quad (5)$$

where h_z is the local heat transfer coefficient and is given by

$$h_z = q_z / (T_w - T_f) \quad (6)$$

The average Nusselt number is given by

$$Nu_{avg} = \frac{1}{L} \int_0^L Nu_z . dz \quad (7)$$

RESULTS AND DISCUSSION

The substrate thickness is varied (1.2-3 mm) while the channel height is maintained constant at 0.6 mm such that the substrate thickness δ_s (below channel) to channel height (δ_f) ratio δ_{sf} varies from 1 to 5. This will help to understand the effect of wall or substrate thickness on conjugate heat transfer. The wall conductivity and flow rate is also varied such that k_{sf} = 0.34-646, and Re = 100-500. Thus, the parametric variations include δ_{sf}, k_{sf} and Re. In the geometry under consideration, only one channel wall is parallel to the surface on which constant wall heat flux is applied, while the remaining two channel walls are perpendicular to it. This makes the heat transfer in transverse direction a two dimensional in nature. As the thickness of the solid substrate increases, the fully

heated boundary moves away from the actual solid-fluid interface. Ideally, it is expected that there is no axial variation of wall heat flux at the solid-fluid interface as uniform heat flux is applied over the whole bottom surface of the substrate. Higher substrate thickness causes higher solid cross-section area, thus scope for higher axial wall conduction. As heat flows by conduction in a direction opposite to that of fluid, the heat flux near the inlet will likely to be higher than near the outlet. This will indicate influence of axial wall conduction. Considering this, the axial variation of dimensionless local heat flux at the solid-fluid interface (ϕ) is presented in Fig. 2 for different Re, k_{sf} and δ_{sf}. The ideal value of ϕ should be equal to unity throughout the length of the channel, which is shown in Fig. 2 by a horizontal dotted line. It is clear from Fig. 2 that the actual heat flux affecting at the solid-fluid interface irrespective of the conductivity ratio, thickness ratio and flow rate. At low k_{sf} (Fig. 2a) dimensionless local heat flux holds an ideal value except at the peak of the channel for all the values of δ_{sf}. This happen due to wavy passage and boundary layers shifted from the centre line towards the peak which is clearly indicated in Fig. 2. Hence the variation of ϕ is in a wavy form along the channel length for the value of k_{sf}, δ_{sf} and flow Re. Secondly at higher k_{sf} (Fig. 2(c)), dimensionless local heat flux (ϕ) deviates from the ideal value and continuously decreases towards the outlet. The deviation of ϕ also increases with δ_{sf}. This indicates the dominance of axial wall conduction at these situations. As the Re value increased to 500 (see Fig. 2 (d,e,f)), it can be observed that hydrodynamic and thermal boundary layers are thinned due to wavy passage and the waviness of the ϕ drops down at the peak and move towards the ideal value for all value of k_{sf} and δ_{sf}. So here flow Re plays an important to role to reduce the dominance of axial wall conduction.

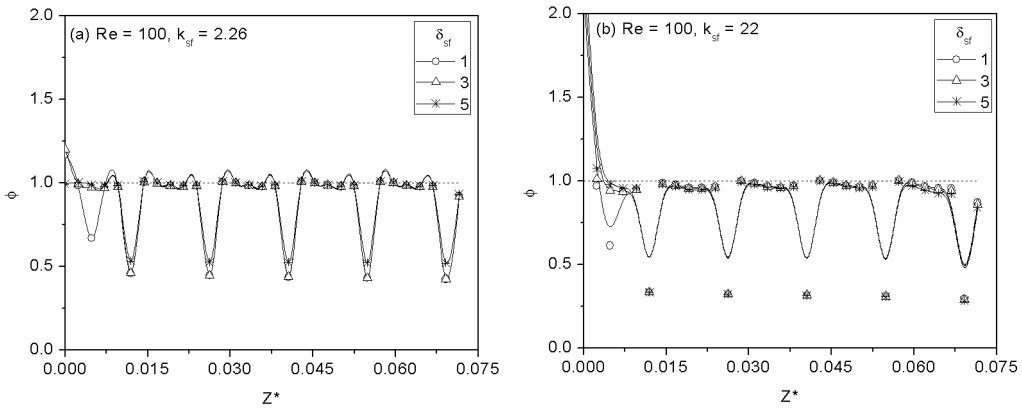

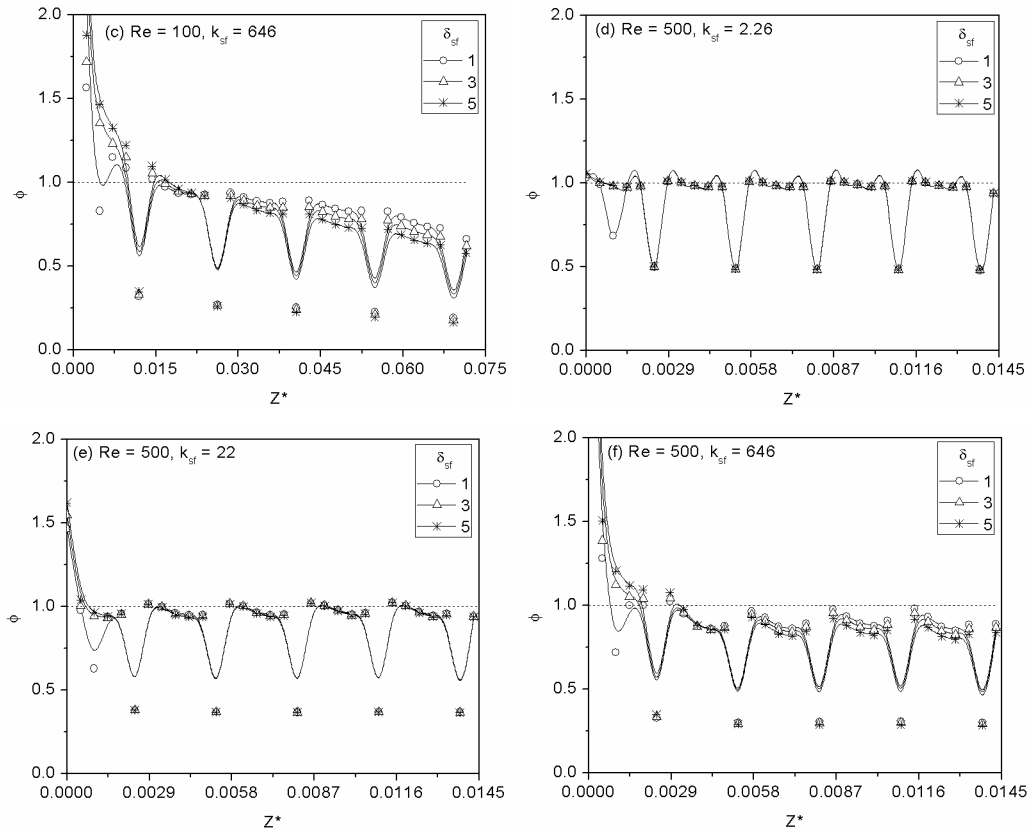

FIGURE 2. VARIATION OF DIMENSIONLESS WALL HEAT FLUX

Fig. 3 shows the axial variation of dimensionless wall and bulk fluid temperature as a function of k_{sf}, Re and δ_{sf}. In Fig 3a (low k_{sf}), the wall and fluid temperature rise as per the conventional theory applicable for the zero wall thickness subjected to the constant wall heat flux boundary condition and after reaching in fully developed condition the wall and fluid temperature difference (Θ_w-Θ_f) attains a constant value. In Fig. 3 (c, f), this is the case in which the difference between the solid wall temperature and fluid wall temperature (solid-fluid interface) is very less, so we can say this is the isothermal condition. And near the inlet region, the wall temperature decreases rapidly. Here we can say that the behavior of plot similar to the conventional theory applicable for the zero wall thickness subjected to the constant wall temperature boundary condition. In fully developed region, the temperature difference (Θ_w-Θ_f) increases with increase in flow Re (Fig. 3 (d, e)). And also with increase in Re, the thermal performance is enhanced which can be observed in Fig. 3 (d).

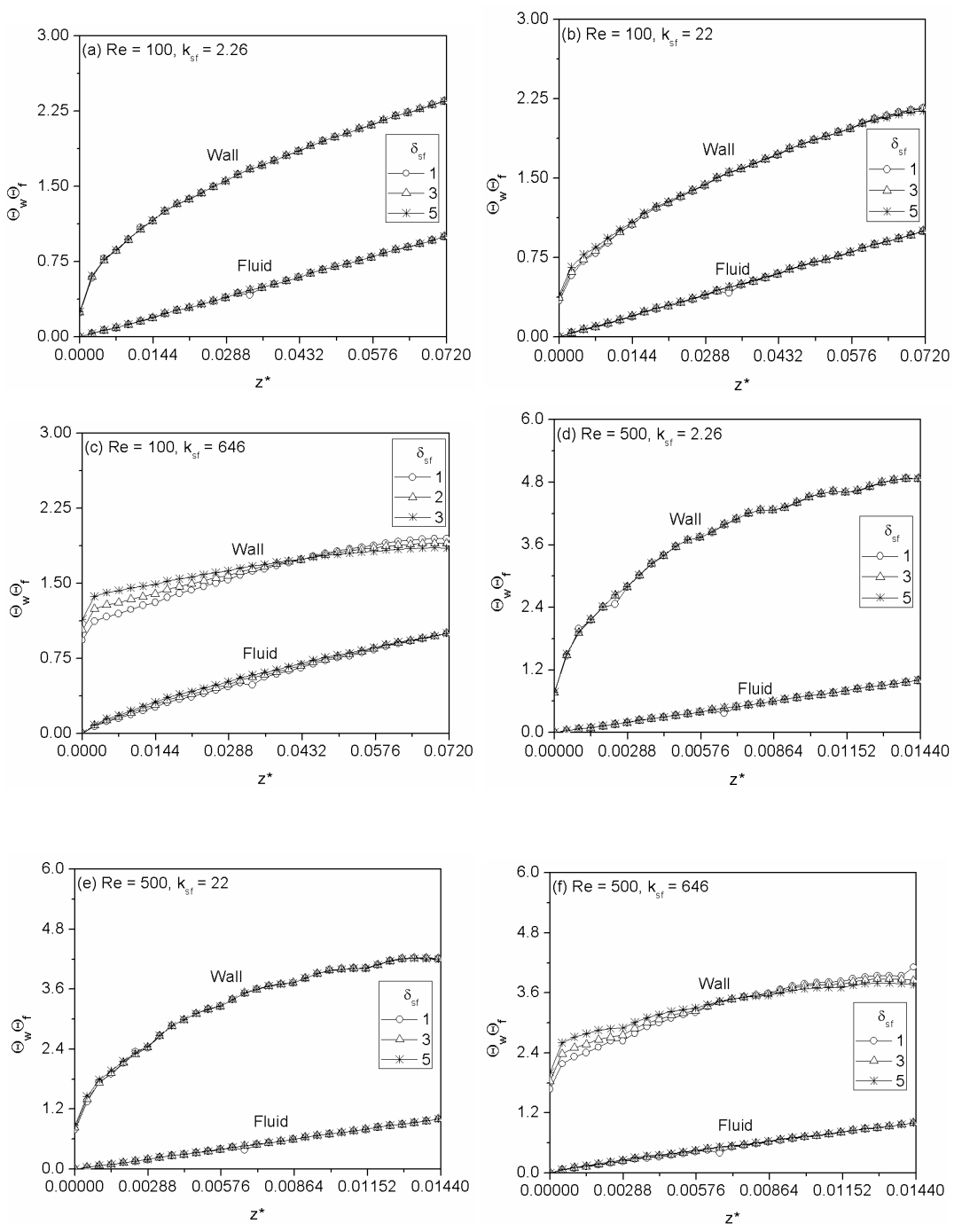

FIGURE 3. VARIATION OF DIMENSIONLESS WALL AND BULK FLUID TEMPERATURE

Fig. 4 shows the axial variation of local Nusselt number subjected to constant wall heat flux boundary condition. Like dimensionless local heat flux, the fully developed Nusselt number is found to be lower at the peak for all value of k_{sf} and δ_{sf} and flow Re. Secondly, at lowest k_{sf} (Fig. 4 (a,d)), fully developed Nu is attains lowest value for all value of δ_{sf}. As the k_{sf} increases, the value of fully developed Nu is increases and at the time

corresponding to the increase in flow Re increases the time to attains the fully developed condition which is clearly shows in Fig. 4 (e, f),. Means that the dominance of the conductivity ratio k_{sf}, in affecting the alteration in the local Nusselt number due to conjugate heat transfer effects, is higher than the thickness ratio δ_{sf}. As already discussed the hydrodynamic and thermal boundary layers are thinned due towavy passage and they shifted from the centerline towards the peak. This biased shift in the centerline velocity was observed to occur with increasing Re = 500. This results in significantly enhanced the thermal performance, which can be observed in Fig. 4 (d,e,f), where the local Nusselt number found to be larger near the peaks compared to low Re = 100 for all value of δ_{sf}. And as the k_{sf} value increased the local Nusselt number were also increases. This helps to decrease the dominance of axial wall conduction. From above discussion we can say the value of local Nusselt number is function of Re and k_{sf}.

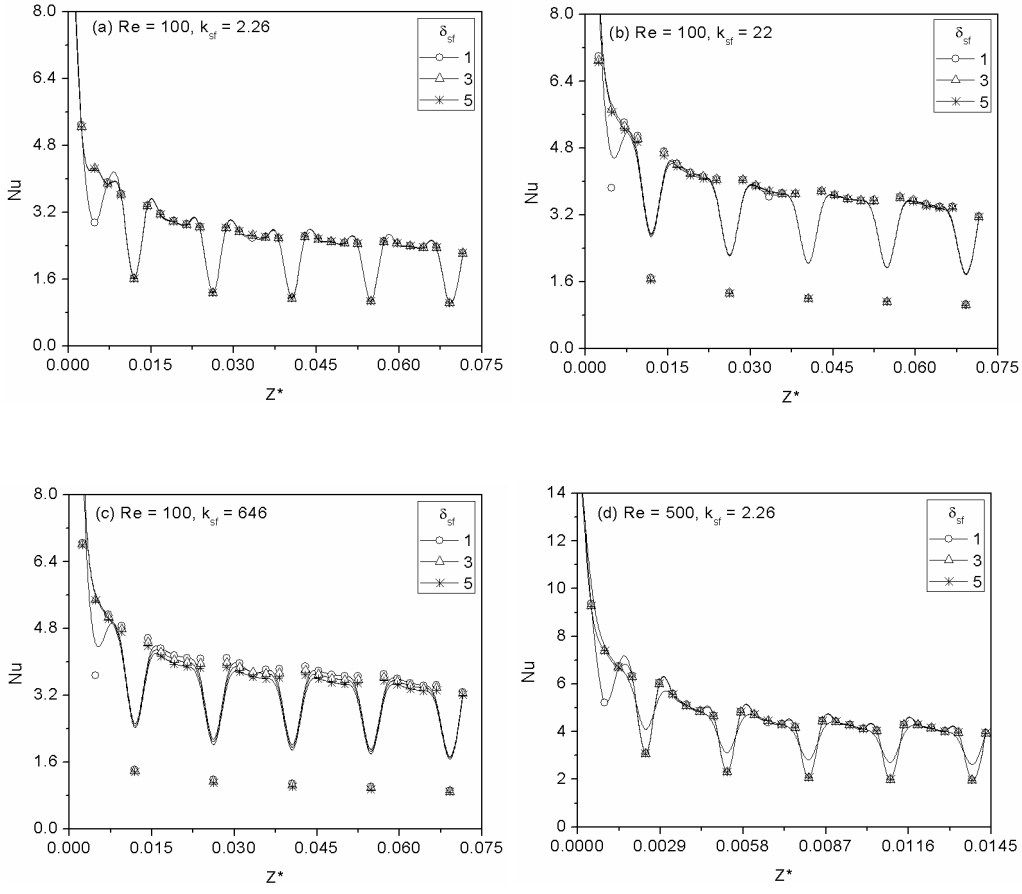

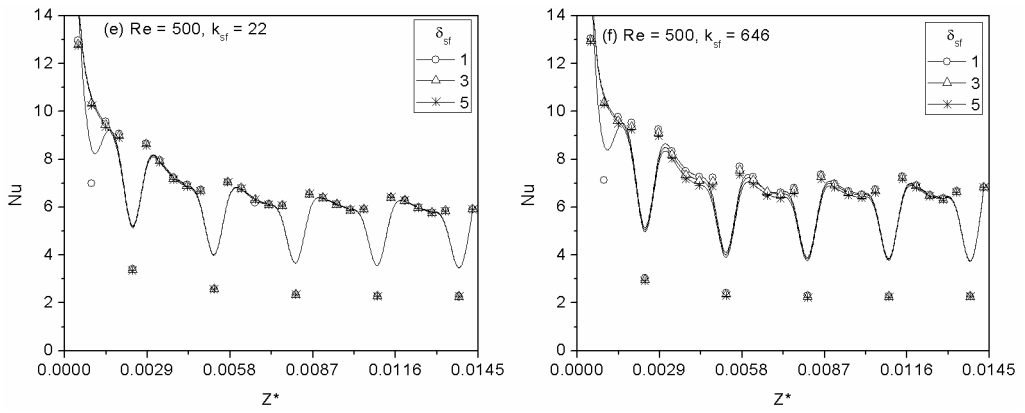

FIGURE 4. VARIATION OF LOCAL NUSSELT NUMBER

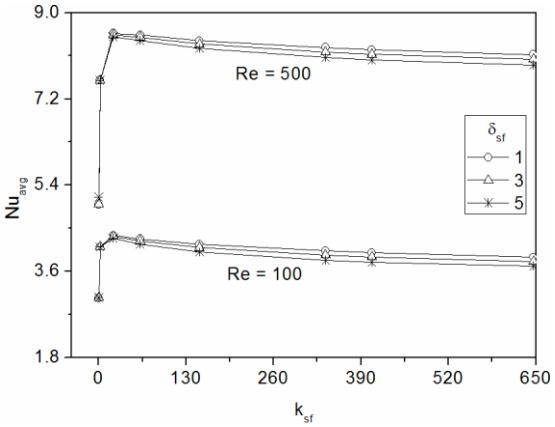

FIGURE 5. VARIATION OF AVERAGE NUSSELT NUMBER WITH CONDUCTIVITY RATIO

Fig. 5 shows the variation of average Nu as defined in Eq. (7) with varying conductivity ratio k_{sf}. For constant wall heat flux approach, it can be observed that at low k_{sf}, the value of Nu_{avg} is small for all thickness ratio (δ_{sf}) and flow Re. Further increase in k_{sf}, Nu_{avg} attains a maximum value and after that the slope goes downward with increasing k_{sf} for all set of δ_{sf} and

Re. This decrease in Nu_{avg} is primarily due to the increasing effect of conjugate heat transfer in the wavy microchannel, leading to axial wall conduction. As flow development length increases with Re, it causes to increase the average Nu while other parameters (k_{sf} and δ_{sf}) are same.

SUMMARY AND CONCLUSION

A numerical study has been carried out to understand the effect of axial wall conduction in conjugate heat transfer situation in a square cross-section wavy microchannel. Simulations have been carried out for a wide

range of substrate wall to fluid conductivity ratio (k_{sf} ~ 0.34 to 646), substrate thickness to channel depth ratio (δ_{sf} ~ 1, 3, and 5), and flow Re (100 to 500). The results clearly show that the dominance of the conductivity ratio k_{sf}, in affecting the alteration in the local Nusselt number due to conjugate heat transfer effects, is higher than the thickness ratio δ_{sf}. The axial conduction alters the condition at the solid-fluid interface more prominently at higher substrate conductivity (k_{sf}) and at lower flow Re. With decreasing k_{sf}, the situation improves. Again, with increasing flow Re, the effect of axial wall conduction decreases. As a result the local Nusselt number for Re = 500 found to be larger near the peaks compared to low Re = 100 for all value of δ_{sf}. And also at k_{sf} = 22, Nu_{avg} attains its maximum value and after that slope goes downward with increasing k_{sf} for all set of δ_{sf} and Re.

NOMENCLATURE

T_w	Wall temperature, K
T_f	Bulk fluid Temperature, K
q_w	Wall heat flux, W/m^2
$\bar{u}$	Average velocity at inlet, m/s
k_s	Solid thermal conductivity, W/mK
k_f	Fluid thermal conductivity, W/mK
c_p	Specific heat of fluid, J/kgK
k_{sf}	Ratio of k_s and k_f
L_s	Total length of substrate, m
L_c	Total length of channel, m
w	Width of the substrate, m
h	Height of the channel, m
h_z	Local heat transfer coefficient, W/m^{2}K
Nu_z	Local Nusselt number
Nu_{avg}	Average Nusselt number
Pr	Prandtl number
Re	Reynolds number
u	Velocity in the axial direction, m/s
q''	Heat flux experienced at the solid-fluid interface of the channel, W/m^2

$\bar{q}$ Heat flux at the bottom surface of the substrate, W/m^2

z Axial coordinate, m

z^* Non dimensional axial coordinate

Greek symbols

δ_f Channel depth, m

δ_s Substrate thickness, m

δ_{sf} Ratio of δ_s and δ_f (-)

μ Dynamic viscosity, Pa-s

ρ Density, kg/m^3

ϕ Non-dimensional local heat flux (-)

Θ Non-dimensional temperature (-)

Subscripts

f Fluid

s Solid

REFERENCES

1. Moharana, M. K., Singh, P. K., and Khandekar, S., 2012, "Optimum Nusselt number for simultaneously developing internal flow under conjugate conditions in a square microchannel," J. Heat Transf., 134 071703, pp. 01-10.
2. Moharana, M. K., Khandekar, S., 2012, "Numerical study of axial back conduction in microtubes," In Proceedings of the Thirty Ninth National Conference on Fluid Mechanics and Fluid Power, December 13-15 (2012), SVNIT Surat, Gujarat, India, Paper number FMFP2012 – 135.
3. Moharana, M. K., and Khandekar, S., 2013, "Effect of aspect ratio of rectangular microchannels on the axial back-conduction in its solid substrate," Int. J. Microscale and Nanoscale Thermal and Fluid Transport Phenomena, 4 (3-4), pp. 1-19.
4. Kumar, M., and Moharana, M. K., 2013, "Axial wall conduction in partially heated microtubes," In: Proceedings of the 22nd National and 11th International ISHMT-ASME Heat and Mass Transfer Conference, IIT Kharagpur, India (2013).
5. Yadav, A., Tiwari, N., Moharana, M. K., and Sarangi, S. K., 2014, "Axial wall conduction in cryogenic fluid microtubes," 4th International and 41th National Conference on Fluid Mechanics and Fluid Power (FMFP2013), (December 2014), Kanpur, India.

6. Mishra, P., and Moharana, M. K., 2014, “Axial wall conduction in pulsating laminar flow in a microtube, 12th International Conference on Nanochannels, Microchannels, and Minichannels,” 3-7 August 2014, Chicago, USA.
7. Wang, L., and Yang, T., 2004, “Bifurcation and stability of forced convection in curved ducts of square cross-section,” Int. J. Heat Mass Transf., 47, pp. 2971-2987.
8. Zhang, S. X., He, Y. L., Lauriat, G., and Tao, W. Q., 2010, “Numerical studies of simultaneously developing laminar flow and heat transfer in microtubes with thick wall and constant outside wall temperature,” Int. J. Heat Mass Transf., 53 (19–20), pp. 3977–3989.
9. Huang, C., Wu, C., Chen, Y., and Liou, T., 2014, “The experimental investigation of axial heat conduction effect on the heat transfer analysis in microchannel flow,” Int. J. Heat Mass Transf., 70, pp. 169–173.
10. Kalb, C. E., and Seader, J. D., 1972, “Heat and mass transfer phenomena for viscous flow in curved circular tubes,” Int. J. Heat Mass Transf., 15 (4), pp. 801-817.
11. Masliyah, J. H., and Nandakuma, K., 1979, “Fully developed viscous flow and heat transfer in curved semi-circular sectors,” AIChE J., 25 (3), pp. 478-487.
12. Rosaguti, N. R., Fletcher, D. F., and Haynes, B. S, 2005, “Laminar flow and heat transfer in a periodic serpentine channel,” Chemical Engg. Tech. 28 (2005) (3) 353-361.
13. Geyer, P. E., Rosaguti, N. R., Fletcher, D. F., and Haynes, B. S., 2006, “Laminar thermo- hydraulics of square ducts following a serpentine channel path,” Microfluid Nanofluid, (3), pp. 195-204.
14. Gong L., Kota, K., Tao, W., and Joshi, Y., 2010, “Parametric Numerical Study of Flow and Heat Transfer in Microchannels with Wavy Walls,” in: ASME 2010 International Mechanical Engineering Congress and Exposition, Vol. 7, Canada (Nov. 2010), 1365-1373.
15. Sui, Y., Teo, C. J., Lee, P. S., Chew, Y. T., Shu, C., 2010, “Fluid flow and heat transfer in wavy microchannels,” Int. J. Heat Mass Transf., 53, pp. 2760-2772.